Studies on the Gust Response of a Wing : Part 1. Response of a Two-Dimensional Rigid Wing

AUTHOR(S):

MAEDA, Hiroshi; KOBAYAKAWA, Makoto

CITATION:

MAEDA, Hiroshi ...[et al]. Studies on the Gust Response of a Wing : Part 1. Response of a Two-Dimensional Rigid Wing. Memoirs of the Faculty of Engineering, Kyoto University 1971, 32(4): 379-404

ISSUE DATE:

1971-01-30

URL:

http://hdl.handle.net/2433/280831

Studies on the Gust Response of a Wing
Part 1. Response of a Two-Dimensional Rigid Wing

By

Hiroshi MAEDA* and Makoto KOBAYAKAWA**

(Received June 30, 1970)

In this report the response characteristics of a two-dimensional, rigid wing (NACA-0012) to the gusts are investigated. The gusts treated here are the normal gusts which vary normal to the main flow sinusoidally and randomly.

In the case of sinusoidal gust, the experimental results show that the absolute value of lift variations are less than those of Sears' function and phase differences are large. In the analyses the thickness effects of airfoil sections are particularly investigated.

In the case of random gust, the generalized harmonic analyses are applied. The frequency transfer functions of lift have the different inclination from those of Sears' function in experimental results. From the power spectral function of circulations the frequency transfer function of lift is obtained analytically and the difference between the experimental results and the calculated ones are discussed.

1. Introduction

One of the most important disturbances on airplanes flying at normal operations is the atmospheric turbulence or the gust. The destruction of airplanes by self-exciting oscillation, such as flutter, may sometimes be caused by the gust. At present airplanes are mostly flying at near sonic speed and high altitude, but the investigation of gust response of airplanes is still important from the standpoint of flight safety, especially in the regions of take-off and landing flight or at relatively low altitude flight. In addition, since high speed airplanes have generally inferior aerodynamic characteristics at low speed, they may easily be affected by the gusts.

The response characteristics of an airplane to several kinds of gusts—such as the step gust, sinusoidal gust, and random gust—have been investigated by many investigators for a long time.[2)~9)] Among the structural components of an airplane, the wing is exceedingly affected by gusts, and therefore it is necessary to investigate the response characteristics of a wing to the gust in detail. Needless to say, the gust response problem is closely related to the non-stationray wing

* Department of Aeronautical Engineering
** Kansai University

theory, and it has been investigated since the time of Theodorsen's theory and developed together with the theory of aeroelasticity.[1] The theory of an oscillating wing with small amplitude in aeroelasticity can easily be converted to the case of a wing in the sinusoidal gust, and this conversion was made by Sears.[5]

Of all kinds of gusts, the most fundamental one is the sinusoidal gust, but of course the actual gusts which airplanes experience vary greatly. In the latter case, the generalized harmonic analysis of random wave, that is, the method of correlations and power spectra, has to be applied.[5),8),10),11),12]

In this study, the gust response problems of a wing will be investigated in detail, and both experimental results and the theoretical analyses about rigid and elastic wings will be presented systematically. In particular the gust response of a two-dimensional rigid wing to sinusoidal and random gusts, which are the most fundamental cases of the problems, are investigated and presented in this report.

2. Sinusoidal Gust Response

2.1 Theoretical Calculations

2.1.1. Response of a Thick Wing

The response of a wing to the gust which varies sinusoidally was given by Sears,[5] and the result is expressed as

$$\frac{|L|}{2\pi\rho b U w_G} = S(k)\, e^{i\omega t} \tag{1}$$

where, L is the lift force and S(k) is called the Sears' gust response function, which is given by

$$S(k) = \frac{J_0(k)K_1(ik) + iJ_1(k)K_0(ik)}{K_1(ik) + K_0(ik)} \tag{2}$$

Equation (1) was obtained under the assumption of thin airfoil and accordingly it may not be applied to thick airfoils exactly. Comparing the theoretically calculated values with experimental results, it is obvious that the experimental data are smaller than the value obtained by equation (1). Since one of the principal reasons for this result is considered to be the effect of the thickness of a wing,

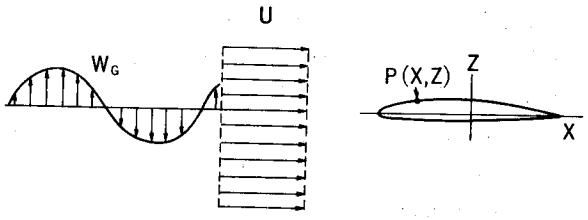

Fig. 1. Wing in gust

it is investigated by reducing the integral equations of circulations with the exact boundary conditions of the thickness of the wing, and solving them numerically.

In the co-ordinate system shown in figure 1, x-axis is taken along the wing chord and the origin on the center of this chord, and therefore an arbitrary point $P(x, z)$ on the airfoil surface can be expressed by,

$$z=\sum_{j=0}^{n} a_j x^j \pm \tau(x) \tag{3}$$

The first term of the right hand side of the above equation expresses m.c.l. (mean camber line) and the second term the thickness of the airfoil (positive sign means the upper surface and negative sign the lower surface).

The airflow around the airfoil consists of the uniform flow U, the gust w_G which is normal to U, and the flow induced by circulations $\gamma_a(\xi, \zeta, t)$ and $\gamma_w(x, t)$ and sources $h(\xi, \zeta, t)$ where γ_a and h are distributed on m.c.l., and γ_w are on the wake shed from the trailing edge. Physically γ_a and h tend to zero at $\xi=b$, and ζ is given by $\sum_{j=0}^{n} a_j \xi^j$.

The induced velocities by the above-mentioned flow on $P(x, z)$ are given by

$$\left.\begin{aligned} u(x,z,t) &= \frac{1}{2\pi}\int_{-b}^{b} \frac{(z-\zeta)\gamma_a(\xi,\zeta,t)}{[(x-\xi)^2+(z-\zeta)^2]}d\xi \\ &\quad + \frac{1}{2\pi}\int_{-b}^{b} \frac{(x-\xi)h(\xi,z,t)}{[(x-\xi)^2+(z-\zeta)^2]}d\xi + \frac{1}{2\pi}\int_{b}^{\infty} \frac{z\gamma_w(\xi,t)}{[(x-\xi)^2+\zeta^2]}d\xi \\ w(x,z,t) &= \frac{1}{2\pi}\int_{-b}^{b} \frac{(x-\xi)\gamma_a(\xi,\zeta,t)}{[(x-\xi)^2+(z-\zeta)^2]}d\xi \\ &\quad + \frac{1}{2\pi}\int_{-b}^{b} \frac{(z-\zeta)h(\xi,\zeta,t)}{[(x-\xi)^2+(z-\zeta)^2]}d\xi + \frac{1}{2\pi}\int_{b}^{\infty} \frac{(x-\xi)\gamma_w(\xi,t)}{[(x-\xi)^2+\zeta^2]}d\xi \end{aligned}\right\} \tag{4}$$

and accordingly the boundary conditions

$$\left.\begin{aligned} \frac{\partial z_U}{\partial x} &= \frac{w_G(x,t)+w(x,z,t)_{z=z_U}}{U+u(x,z,t)_{z=z_U}} \\ \frac{\partial z_L}{\partial x} &= \frac{w_G(x,t)+w(x,z,t)_{z=z_L}}{U+u(x,z,t)_{z=z_L}} \end{aligned}\right\} \tag{5}$$

should be satisfied on the upper- and lower-surface respectively.

Substituting equations (3) and (4) into (5), the following integral equations are obtained.

$$\begin{aligned} &\left(\sum_{j=0}^{n} j a_j x^{j-1} + \frac{d\tau}{dx}\right)U - w_G(x,t) \\ &= -\frac{1}{2\pi}\int_{-b}^{b}\left[\frac{\gamma_a(\xi,\zeta,t)}{(x-\xi)^2+(z-\zeta_U)^2}\left\{(x-\xi)+\left(\sum_{j=0}^{n} j a_j x^{j-1}+\frac{d\tau}{dx}\right)(z_U-\zeta)\right\}\right. \\ &\quad \left. + \frac{1}{2}\frac{h(\xi,\zeta,t)}{\{(x-\xi)^2+(z-\zeta_U)^2\}^{3/2}}\left\{(z_U-\zeta)-\left(\sum_{j=0}^{n} j a_j x^{j-1}+\frac{d\tau}{dx}\right)(x-\xi)\right\}\right]d\xi \\ &\quad - \frac{1}{2\pi}\int_{b}^{\infty}\frac{\gamma_w(\xi,t)}{(x-\xi)^2+z_U^2}\left\{(x-\xi)+\left(\sum_{j=0}^{n} j a_j x^{j-1}+\frac{d\tau}{dx}\right)z_U\right\}d\xi \end{aligned} \tag{6a}$$

$$\left(\sum_{j=0}^{n} j a_j x^{j-1} - \frac{d\tau}{dx}\right) U - w_G(x,t)$$
$$= -\frac{1}{2\pi}\int_{-b}^{b}\left[\frac{\gamma_a(\xi,\zeta,t)}{(x-\xi)^2+(z_L-\zeta)^2}\left\{(x-\xi)+\left(\sum_{j=0}^{n} j a_j x^{j-1}-\frac{d\tau}{dx}\right)(z_L-\zeta)\right\}\right.$$
$$\left.+\frac{1}{2}\frac{h(\xi,\zeta,t)}{\{(x-\xi)^2+(z-\zeta_L)^2\}^{3/2}}\left\{(z_L-\zeta)-\left(\sum_{j=0}^{n} j a_j x^{j-1}-\frac{d\tau}{dx}\right)(x-\xi)\right\}\right]d\xi$$
$$-\frac{1}{2\pi}\int_{b}^{\infty}\frac{\gamma_w(\xi,t)}{(x-\xi)^2+\zeta_L^2}\left\{(x-\xi)+\left(\sum_{j=0}^{n} j a_j x^{j-1}-\frac{d\tau}{dx}\right)z_L\right\}d\xi \qquad (6b)$$

If the shape of the airfoil section is given, a_j and τ can be determined, and also if it is assumed that the gust w_G varies sinusoidally, i.e.

$$w_G = w_G e^{-ik x^*} \cdot e^{i\omega t} \qquad (7)$$

γ_a, γ_w and h are expressed by

$$\left.\begin{aligned}\gamma_a(\xi,\zeta,t) &= \bar{\gamma}_a(\xi,\zeta)e^{i\omega t}\\ \gamma_w(\xi,t) &= \bar{\gamma}_w(\xi)e^{i\omega t}\\ h(\xi,\zeta,t) &= \bar{h}(\xi,\zeta)e^{i\omega t}\end{aligned}\right\} \qquad (8)$$

Then one more equation is necessary to solve two integral equations (6a) and (6b) for three unknowns γ_a, γ_w and h, or to obtain the response of a thick wing.

Since the simultaneous integral equations, (6a) and (6b), are complicated and cannot be treated easily, the shape of airfoil section is divided into two parts,

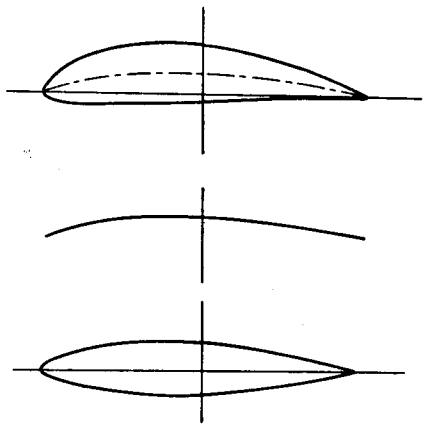

Fig. 2. Decomposition of wing

i.e. (1) symmetrical airfoil, and (2) thin cambered airfoil, as shown in figure 2. Accordingly the solution of the integral equations can be obtained by superimposing each solution.* In the case of the symmetrical airfoil, equation (3) is expressed by

$$\sum_{j=0}^{n} j a_j x^{j-1} = 0, \quad z_U = -z_L = \tau \qquad (9)$$

* Since the latter case, or a thin cambered airfoil, has already been analysed by several workers, the former, or a symmetric thick airfoil, is treated here.

and, therefore, the integral equations, (6a) and (6b), become the following two equations which include only the circulations and the source respectively,

$$-\bar{w}_a e^{-ik\alpha^*} = -\frac{1}{2\pi}\int_{-1}^{1} \frac{\gamma_a(\xi^*)}{(x^*-\xi^*)^2+\tau^{*2}}\left[(x^*-\xi^*)+\tau^*\frac{d\tau^*}{dx^*}\right]d\xi^* - \frac{1}{2\pi}\int_{1}^{\infty} \frac{\gamma_w(\xi^*)}{(x^*-\xi^*)^2+\tau^{*2}}\left[(x^*-\xi^*)+\tau^*\frac{d\tau^*}{dx^*}\right]d\xi^* \tag{10}$$

$$U\frac{d\tau^*}{d\xi^*} = \frac{1}{2\pi}\int_{-1}^{1} \frac{h(\xi^*)}{(x^*-\xi^*)^2+\tau^{*2}}\left[\tau^*-(x^*-\xi^*)\frac{d\tau^*}{d\xi^*}\right]d\xi^* \tag{11}$$

where

$$x^*=x/b,\ \xi^*=\xi/b,\ \zeta^*=\zeta/b,\ \tau^*=\tau/b \tag{12}$$

As mentioned before, the number of unknowns are three in the integral equations, and therefore those equations cannot be solved without one more relation. If the wake vortices are assumed to be shed along x-axis in the same manner as the ordinary thin airfoil theory, another relation is given by

$$\gamma_w(x^*) = -ik\Omega e^{-ik} \tag{13}$$

where, $\Omega=(I'/b)e^{ik}$, $I'(t)=I'e^{i\omega t}$ (14), and $I'(t)$ is the overall circulation of the airfoil. From equation (10), (11) and (13), the circulation and the source distributions of a thick symmetric airfoil can be obtained.

2.1.2 Numerical Calculations for NACA-0012

Although the integral equations (10) and (11) may easily be seen as Fredholm type integral equations of the first kind, the kernels of them are complicated, and in addition τ and ζ which express the shape of the airfoil section are usually given as numerical tables and then it is difficult to solve them analytically.

Therefore, in order to obtain the solutions by a numerical integration method, it is assumed that the circulation and source distributions are expressed by the series form. By substituting them into the integral equations, one-dimensional simultaneous equations for the coefficients as unknowns are obtained and solved numerically. Pressure distribution and the lift can be obtained by the following relations.

$$-\frac{\Delta\bar{p}_a(x,z)}{\rho U} = \bar{\gamma}_a(x,z)+\frac{ik}{b}\int_{-b}^{b}\bar{\gamma}_a(\xi,z)\,d\xi \tag{15}$$

$$\bar{L}=\int_{-b}^{b}\Delta\bar{p}_a(x,z)\,dx \tag{16}$$

where

$$\Delta p_a(x,z,t)=\Delta\bar{p}_a(x,z)e^{i\omega t},\ L(t)=\bar{L}e^{i\omega t} \tag{17}$$

In order to compare them with the experimental results, the solution of equations (10) and (11) is calculated for NACA-0012 airfoil section.

Substituting equation (13) into (10), and using the following relation

$$\bar{\Omega}=(\bar{I}'/b)e^{ik}=e^{ik}\int_{-1}^{1}\bar{\gamma}_a(\xi^*)\,d\xi^* \tag{18}$$

the integral equation to determine $\bar{\gamma}_a(x^*)$ is obtained as follows:

$$-\bar{w}_a \cdot e^{-ikx^*} = -\frac{1}{2\pi}\int_{-1}^{1}\left[\frac{x^*-\xi^*+\tau^*\dfrac{d\tau^*}{dx^*}}{(x^*-\xi^*)^2+\tau^{*2}} - ike^{ik}\int_1^\infty \frac{e^{-ik\xi_1^*}}{(x^*-\xi_1^*)^2+\tau^{*2}} \times\left\{\{x^*-\xi_1^*+\tau^*\frac{d\tau^*}{dx^*}\}\, d\xi_1^*\right]\bar{\gamma}_a(\xi^*)\, d\xi^* \tag{19}$$

To solve this equation, following new variables are introduced.

$$x^* = -\cos\phi,\ \xi^* = -\cos\theta,\ 0 \leqq \theta,\ \phi \leqq n \tag{20}$$

Furthermore, the airfoil is divided into n pieces along the chord line, which are given by the following equations (see figure 3)

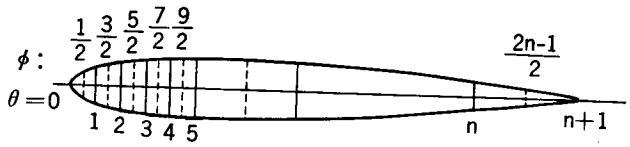

Fig. 3. Division of wing

$$\phi = \frac{(2r-1)\pi}{2n},\ \theta = \frac{(r-1)\pi}{n},\ r = 1, \cdots, n \tag{21}$$

In order to satisfy Kutta's condition, $\gamma_a(\theta)$ is assumed to be[14]

$$\bar{\gamma}_a(\theta) = G_0 \cot\frac{\theta}{2} + \sum_{r=1}^{n-1} G_r \sin r\theta \tag{22}$$

Substituitng those relations into equation (19)

$$-\bar{w}_a e^{ik\cos\phi} = -\frac{1}{2\pi}\int_0^\pi\left[\frac{\cos\theta-\cos\phi+f\cdot f'}{(\cos\theta-\cos\phi)^2+f^2} + ike^{ik}\int_1^\infty \frac{e^{-ik\xi_1^*}}{(\xi_1^*+\cos\phi)^2+f^2} \times\{\xi_1^*+\cos\phi - f\cdot f'\}\, d\xi_1^*\right]\left(G_0\cot\frac{\theta}{2}+\sum_{r=1}^{n-1}G_r\sin r\theta\right)\sin\theta\, d\theta \tag{23}$$

where $f=\tau^*(\phi)$ and $f'=d\tau^*/d\phi$. Equation (23) can be converted into the following simultaneous equations, in which the divided points are given by equation (21),

$$\begin{pmatrix} A_{1,0} & A_{1,1} & \cdots & A_{1,n-1} \\ A_{2,0} & A_{2,1} & \cdots & A_{2,n-1} \\ \cdots & \cdots & \cdots & \cdots \\ A_{n,0} & A_{n,1} & \cdots & A_{n,n-1} \end{pmatrix} \begin{pmatrix} G_0 \\ G_1 \\ \vdots \\ G_{n-1} \end{pmatrix} = \begin{pmatrix} \bar{w}_a e^{ik\cos\phi_1} \\ \bar{w}_a e^{ik\cos\phi_2} \\ \vdots \\ \bar{w}_a e^{ik\cos\phi_n} \end{pmatrix} \tag{24}$$

where

$$\left.\begin{aligned} A_{j,0} &= \frac{1}{2\pi}\int_0^\pi\left\{\frac{\cos\theta-\cos\phi_j+f_j\cdot f_j'}{(\cos\theta-\cos\phi_j)^2+f_j^2}+ikP(\phi_j)\right\}\sin\theta\cot\frac{\theta}{2}d\theta \\ A_{j,r} &= \frac{1}{2\pi}\int_0^\pi\left\{\frac{\cos\theta-\cos\phi_j+f_j\cdot f_j'}{(\cos\theta-\cos\phi_j)^2+f_j^2}+ikP(\phi_j)\right\}\sin\theta\sin r\theta d\theta \\ P(\phi_j) &= \int_1^\infty \frac{e^{-ik\xi_1^*}}{(\xi_1^*+\cos\phi_j)^2+f_j^2}\{\xi_1^*+\cos\phi_j+f_j\cdot f_j'\}\, d\xi_1^*\cdot e^{ik} \end{aligned}\right\} \tag{25}$$

In order to solve the simultaneous equations (24), the sweepout method is

applied, in which the number of dividing points are 60 (n=60) in this calculation, and the section ordinates f and their derivatievs or gradients f' can be obtained from the following equations

$$\left.\begin{aligned} f &= 7.56\times10^{-4}\ (0.857\sqrt{x}-1.050x-24.417x^2+164.525x^3-489.486x^4) \\ f' &= 7.56\times10^{-4}\ (0.429/\sqrt{x}-1.050-48.834x+553.576x^2-1957.944x^3) \end{aligned}\right\} \tag{26}$$

The digital computer, FACOM 230–60 at Kyoto university, was used to determine the numerical calculations. The results are illustrated in figure 4 (circulation distributions) and 5 ($|\bar{L}|/(2\pi\rho bUw_0)$). The former can be obtained by equation (22), and the latter by the following equations,[4]

$$\begin{aligned} \frac{\bar{L}}{2\pi\rho bUw_0} &= -\int_{-1}^{1} \Delta p_a(x^*)\,dx^* \\ &= \int_{-1}^{1} \gamma_a(x^*)\,dx^* + ik\int_{-1}^{1} dx^* \int_{-1}^{x^*} \gamma_a(\xi^*)\,d\xi^* \\ &= \left(\frac{1}{2}+\frac{I_0}{2\pi}-ik\right)G_0+\frac{1}{4\pi}\sum_{r=1}^{n-1} I_r G_r \end{aligned} \tag{27}$$

where

$$\left.\begin{aligned} I_0 &= \int_0^{\pi} \sin\ (\cos\phi)\ \sin\phi\ d\phi \\ I_r &= \frac{1}{r+1}\int_0^{\pi} \sin\ [(r+1)\cos\phi]\ \cos\phi d\phi \\ &\quad -\frac{1}{r-1}\int_0^{\pi} \sin\ [(r-1)\ \cos\phi]\ \sin\phi d\phi \end{aligned}\right\} \tag{28}$$

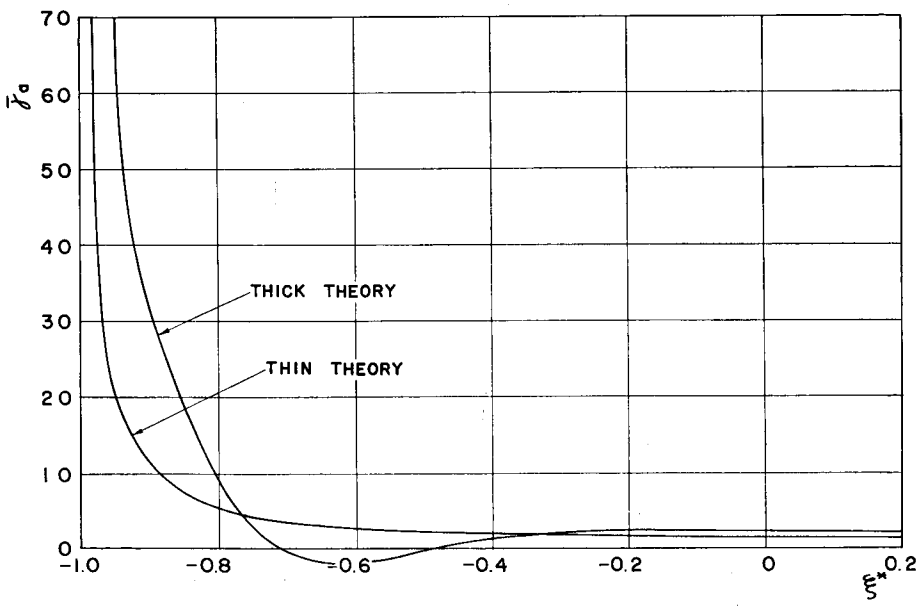

Fig. 4. Circulation of thick airfoil theory (k=0.01)

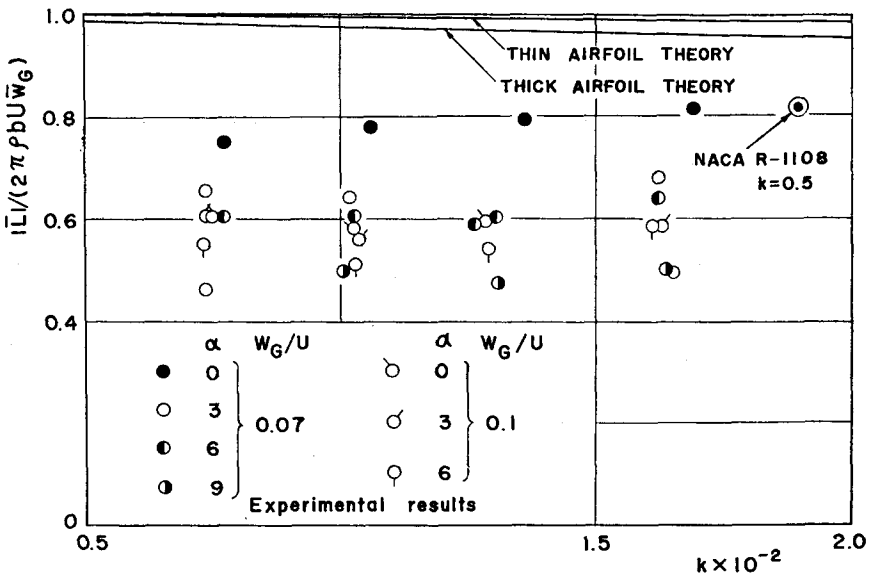

Fig. 5. Nonsteady effects

The differences between those results and the thin airfoil theory are obvious in figure 4 and 5.

2.2. Experiments

The experiments for determining the response of a wing to the gust varying sinusoidally were carried out in a low speed wind tunnel.

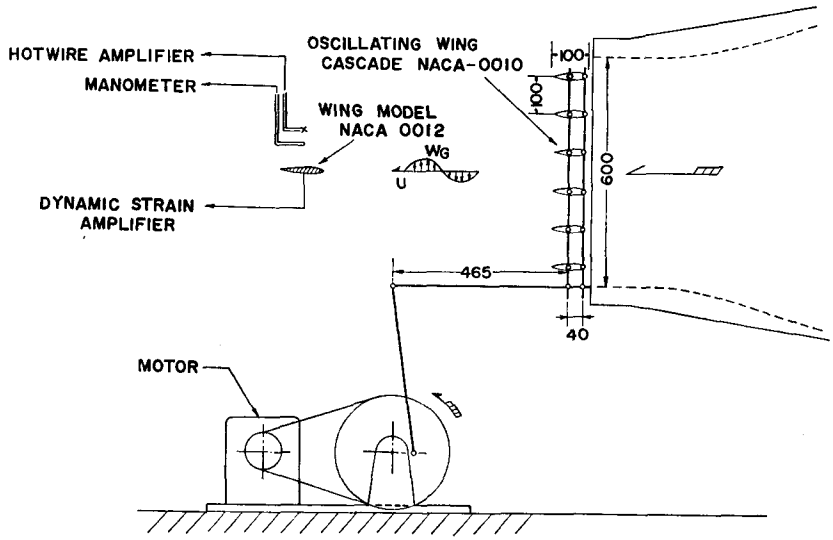

Fig. 6. Side view of apparatus

2.2.1. Experimental Apparatus

The sinusoidal gust is produced by an oscillating wing cascade (each airfoil section is NACA-0010) which was set on the effuser's exit of the wind tunnel as shown in figure 6. This cascade wing can be oscillated by a simple crank mechanism having the axis of rotation at the center of chord. With this crank mechanism, the variation of angle of attack of cascade wings cannot become the exact sinusoidal oscillation, but it is confirmed that the error is negligible when the crank arm is long compared with the amplitude of cascade oscillation.

As shown in figure 9, the variations of flow velocity w_G, which were measured at a point of 600 mm downstream of the cascade, are satisfactorily considered to be a sinusoidal variation.

The other experimental apparatus is also shown in figure 6. The wind tunnel used for this experiment is a low speed blow down type, having a working

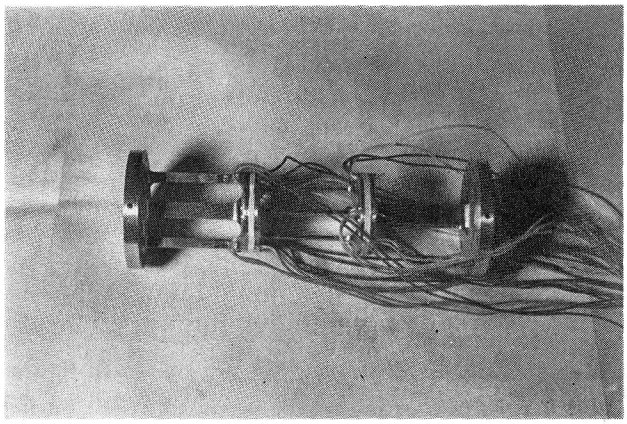

Fig. 7. Strain gage balance

section of square shape (600 mm × 600 mm), the maximum flow velocity is about 30 m/s, and the turbulence intensity is less than 0.06% r.m.s. at the direction of main flow. The model chord length and the span are 120 mm and 512 mm respectively, and to satisfy the two-dimensionality condition, two side plates are equipped. The airfoil section is NACA-0012. The wing is supported at both wing tips by the strain gage balance which is used to measure the lift, drag and pitching moment (see figure 7). The balance has quite small interferences between each element.

Measurements of the gust were made by using the hot-wire anemometer which is fixed above the model wing. The hot-wire used in this experiment is X-type, and the outputs obtained from each element are u_G (by adding) and w_G (by subtracting) respectively. The values of the measurement are recorded by 6 channel

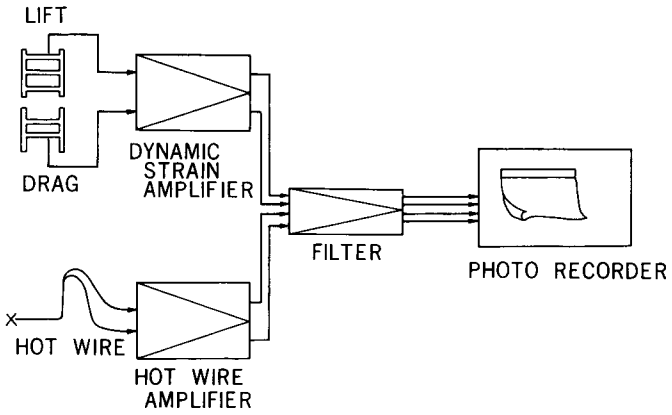

Fig. 8. Block diagram

photo-magnetic oscillograph. In addition, the velocity of uniform flow, U, is measured by a pitot-static tube and a manometer of Göttingen type. The block diagram of those measurements is shown in figure 8.

2.2.2. Experimental Results

Parameters of the experiments are the amplitude of gust w_G, the reduced frequency k $(=\omega b/U)$ and the wing angle of attack α. In our experiments the range of variation of these parameters is as follows:

$\bar{w}_G/U$: 0.01, 0.07

k : 0.007~0.017 (6 points)

α : 0, 3, 6, 9, 12°

Typical records of the gust, lift and drag are shown in figure 9. After converting the lift and drag into C_L and C_D for various k, their variations are shown

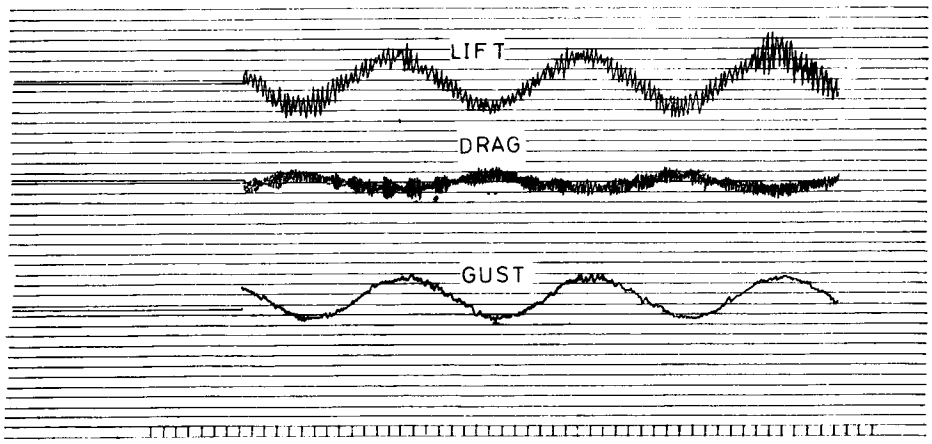

Fig. 9. Typical records of response

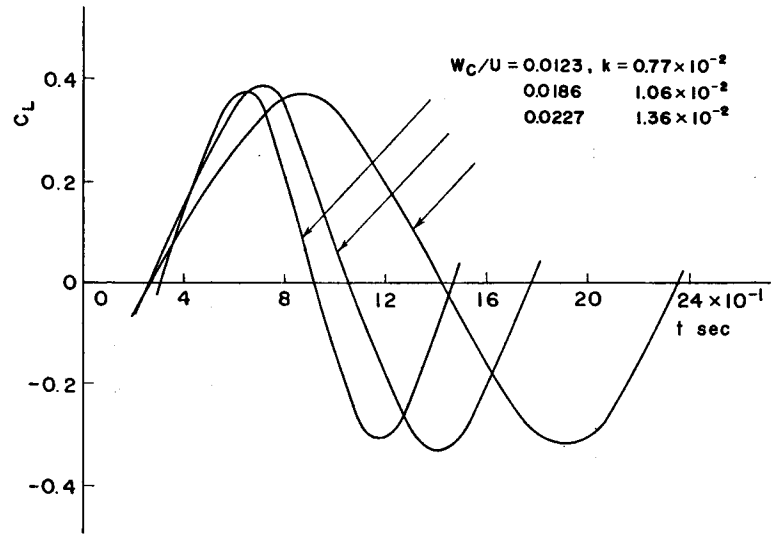

Fig. 10(a). Variation of C_L

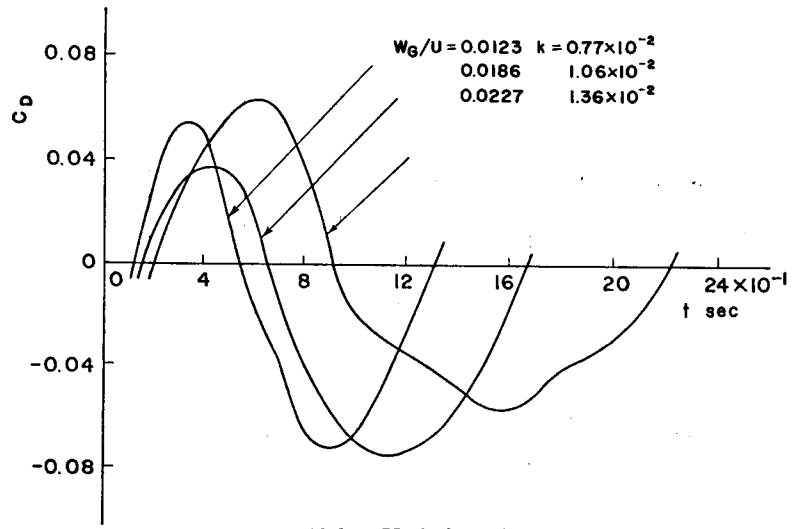

Fig. 10(b). Variation of C_D

in figure 10. From this figure it is found that C_L curves look apparently sinusoidally, but C_D curves get out of shape considerably. Furthermore, the peak to peak values are plotted in figure 11, which shows that they are approximately constant within the range of k.

Phase differences between w_g and C_L or C_D are shown in figure 12, and the non-dimensional lift variation, $\overline{L}/(2\pi\rho bU\overline{w}_g)$, is shown in figure 5.

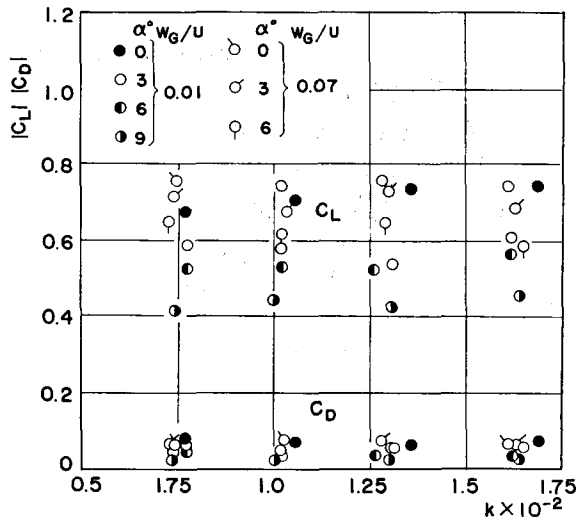

Fig. 11. Peak value of lift, drag

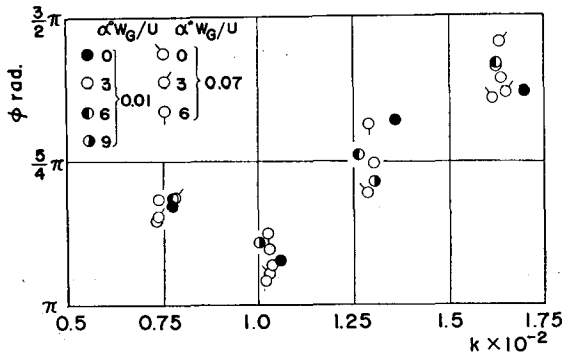

Fig. 12. Phase differences

2.3. Considerations

The lift variation of an airfoil which is immersed in the sinusoidally varying gust shows, as shown in figure 5, that the experimental values are far below that of the value calculated with the stationary thin airfoil theory. The experimental results obtained by R.L.Halfman for an oscillating wing with the section of NACA-0012 also show that the lift coefficients are smaller when k is small.[7] The experimental values, however, agree with theoretical value when k is larger. Accordingly, the reasons are as follows:

(a) When k is small, the viscous effects become larger than the non-stationary effects.

(b) The lift decreases by the thickness effect (see figure 5).

Among these effects the thickness effect has been discussed in this chapter, and accordingly the viscous effect should be included for further calculations.

3. Random Gust Response

3.1. Theoretical Caclulations

3.1.1. Random Process

The statistical method must be utilized to investigate the response of a wing to the gust which varies randomly.[9] This is the application of techniques which are frequently used in the studies of random process, such as noise. In order to apply this technique, the following assumptions are presented, i.e.

(a) Variations of all the quantities, such as gust, lift, drag etc., are stationary random processes.

(b) These processes are ergodic processes. Therefore, the time correlation is equal to the space correlation.

Utilizing those assumptions, there exists the mean square value for random variable $y(t)$ defined by the following equation,

$$\overline{y^2(t)}=\lim_{T\to\infty}\frac{1}{T}\int_0^T[y(t)]^2dt \tag{30}$$

If this value can be considered to be the mean energy, and the composite of infinitely many frequency components, $\overline{y^2(t)}$ can be expressed by the power spectral function,

$$\overline{y^2(t)}=\int_0^\infty \Phi(\omega)\,d\omega \tag{31}$$

where

$$\Phi(\omega)=\lim_{T\to\infty}\frac{1}{\pi T}\left|\int_0^T y(t)\,e^{-i\omega t}dt\right|^2 \tag{32}$$

Power spectral function $\Phi(\omega)$ can be related to auto-correlation function $R(\tau)$ of $y(t)$ by Fourier transformation which is expressed by

$$\left.\begin{aligned}\Phi(\omega)&=\frac{2}{\pi}\int_0^\infty R(\tau)\,e^{-i\omega\tau}d\tau\\ R(\tau)&=\int_0^\infty \Phi(\omega)\,e^{i\omega\tau}d\omega\end{aligned}\right\} \tag{33}$$

With the application of the above-mentioned treatment, it is possible to investigate the response of a wing to the random gusts.

3.1.2. Response to Random Gust

Among the responses to the random gust, the lift can be calculated by the circulation distributions in the same manner as the case of the sinusoidal gust. At first, it is assumed that

(a) The wing is a thin airfoil and it can be replaced by a circulation dis-

tribution.

(b) The airflow is incompressible and disturbances are propagated simultaneously.

(c) The gusts are two-dimensional.

The integral equation for circulation distributions holds also for the random gust at an arbitrary instant as follows:

$$w_G(x,t)=\frac{1}{2\pi}\left[\oint_{-b}^{b}\frac{\gamma_a(\xi^*,t)}{x^*-\xi^*}d\xi^*+\int_{b}^{\infty}\frac{\gamma_w(\xi'^*,t)}{x^*-\xi'^*}d\xi'^*\right] \tag{34}$$

Where $\gamma_a(\xi^*,t)$ and $\gamma_w(\xi^*,t)$ are unknowns in the above equation, but since the latter can be expressed by $w_G(x^*,t)$ with the relation at the trailing edge, it is considered to be the known quantity.

Therefore, applying the Söhngen's relation[1]

$$\gamma_a(x^*,t)=-\sqrt{\frac{2}{\pi}}\frac{1-x^*}{1+x^*}\oint_{-1}^{1}\frac{1+\xi^*}{1-\xi^*}\frac{1}{x^*-\xi^*}\left[w_G(\xi^*,t)+\frac{1}{2\pi}\int_{1}^{\infty}\frac{\gamma_w(\lambda,t)}{\xi^*-\lambda}d\lambda\right]d\xi^* \tag{35a}$$

The variables, w_G, γ_a, and γ_w, vary randomly, but it is considered that equation (35a) holds at an arbitrary instant. Then at time $t+\tau$,

$$\gamma_a(x_1^*,t+\tau)=-\sqrt{\frac{2}{\pi}}\frac{1-x_1^*}{1+x_1^*}\oint_{-1}^{1}\frac{1+\xi_1^*}{1-\xi_1^*}\frac{1}{x_1^*-\xi_1^*}\times\left[w_G(\xi_1^*,t+\tau)+\frac{1}{2\pi}\int_{1}^{\infty}\frac{\gamma_w(\lambda_1,t+\tau)}{\xi_1^*-\lambda_1}d\lambda_1\right]d\xi_1^* \tag{35b}$$

If above two-equations, (35a) and (35b), are multiplied side by side and integrated from t to T, the auto-correlation function can be obtained at the limit of $T\to\infty$,

$$R_{\gamma a}(x^*,x_1^*,\tau)=\frac{4}{\pi^2}\frac{1-x^*}{1+x^*}\frac{1-x_1^*}{1+x_1^*}\oint_{-1}^{1}\oint_{-1}^{1}\frac{1+\xi^*}{1-\xi^*}\frac{1}{(x^*-\xi^*)\ (x_1^*-\xi_1^*)}\times\Bigg[R_{wG}(\xi^*,\xi_1^*,\tau)+\frac{1}{(2\pi)^2}\Bigg\{\int_{1}^{\infty}\int_{1}^{\infty}\frac{R_{\gamma w}(\lambda,\lambda_1,\tau)}{(\xi^*-\lambda)\ (\xi_1^*-\lambda_1)}d\lambda d\lambda_1+\int_{1}^{\infty}\frac{R_{wG\gamma w}(\xi^*,\lambda_1,\tau)}{\xi_1^*-\lambda_1}d\lambda_1+\int_{1}^{\infty}\frac{R_{\gamma wG}(\xi_1^*,\lambda,\tau)}{\xi^*-\lambda}d\lambda\Bigg\}\Bigg]d\xi^*d\xi_1^* \tag{36}$$

The reason why x^* and x_1^* are chosen as the variables in equation (36) depends on the convenience of integration. However, since w_G and γ_w are shed away with velocity U, the correlation interval and its position should be as follows: (see figure 13)

$$\lim_{T\to\infty}\frac{1}{T}\int_{-T}^{T}\left\{\oint_{-1}^{1}\frac{1+\xi^*}{1-\xi^*}\frac{w_G(\xi^*,t)}{x^*-\xi^*}d\xi^*\right\}\left\{\oint_{-1}^{1}\frac{1+\xi_1^*}{1-\xi_1^*}\frac{w_G(\xi_1^*,t+\tau)}{x_1^*-\xi_1^*}d\xi_1^*\right\}dt$$
$$=\oint_{-1}^{1}\oint_{-1}^{1}\frac{1+\xi^*}{1-\xi^*}\frac{1+\xi_1^*}{1-\xi_1^*}\frac{d\xi^*d\xi_1^*}{(x^*-\xi^*)\ (x_1^*-\xi_1^*)}\left\{\lim_{T\to\infty}\frac{1}{T}\int_{-T}^{T}w_G(\xi^*,t)\ w_G\left(\xi^*,t+\tau-\frac{\xi_1^*-\xi^*}{U}\right)dt\right\}$$

$$\therefore\quad R_{wG}(\xi^*,\xi_1^*,\tau)=\lim_{T\to\infty}\frac{1}{T}\int_{-T}^{T}w_G(\xi^*,t)\ w_G\left(\xi^*,t+\tau+\frac{\xi_1^*-\xi^*}{U}\right)dt \tag{37}$$

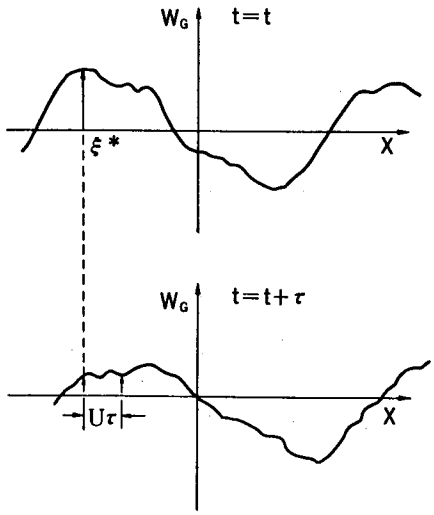

Fig. 13. Correlation of gust

in the same manner, for γ_w

$$R_{\gamma w}(\lambda, \lambda_1, \tau) = \lim_{T\to\infty} \frac{1}{T}\int_{-T}^{T} \gamma_w(\lambda, t)\gamma_w\left(\lambda, t+\tau+\frac{\lambda_1-\lambda}{U}\right)dt \tag{38}$$

The relation between the total circulation of airfoil and the wake vortices are given by

$$\int_1^\infty d\lambda_1 \int_1^\infty R_{\gamma w}\left(\lambda, \tau+\frac{|\lambda_1-\lambda|}{U}\right)d\lambda = \frac{1}{b^2}\, R_\Gamma(\tau) \tag{39}$$

or

$$\oint_{-1}^{1} dx_1^* \oint_{-1}^{1} R_{\gamma a}(x^*, x_1^*, \tau)\, dx^* = R_\Gamma(\tau) \tag{40}$$

If the gust is assumed to be homogeneous and isotropic and no correlation between w_G and γ_w exists, $R_{\gamma a}$, $R_{\gamma w}$, and R_Γ can be obtained by equations (36), (37), (38), (39) and (40). However, since these integral equations are complicated, it is difficult to treat analytically. Then another relation beween $R_{\gamma a}$ and R_Γ is introduced as follows:

$$R_{\gamma w}(\lambda, \lambda_1, U\tau) = -k^2\, R_\Gamma(U\tau)\, e^{-ik(\lambda+\lambda_1)} \tag{41}$$

Using this equation, $R_{\gamma a}$ can be calculated from equation (36). Applying the Fourier transformation to the equation of $R_{\gamma a}$, the power spectral function of circulation distribution is obtained as follows:

$$\Phi_{\gamma a}(x^*, x_1^*, k) = \left(\frac{2}{\pi}\right)^2 \sqrt{\frac{1-x_1^*}{1+x_1^*}}\,\sqrt{\frac{1-x^*}{1+x^*}}\,\oint_{-1}^{1}\sqrt{\frac{1+\xi_1^*}{1-\xi_1^*}}\,\frac{d\xi_1^*}{x_1^*-\xi_1^*}\oint_{-1}^{1}\sqrt{\frac{1+\xi^*}{1-\xi^*}}$$
$$\frac{1}{x^*-\xi^*}\times\left\{\left[e^{-ik_1(\xi_1^*-\xi^*)}\Phi_G(k) - \frac{k_1}{2}(\xi_1^*-\xi^*)e^{-ik_1(\xi_1^*-\xi^*)}\Phi_F(k)\right]\right.$$
$$\left.-\left(\frac{k}{2\pi}\right)^2 \Phi_\Gamma(k)\int_1^\infty \frac{d\lambda_1}{\xi_1-\lambda_1}\int_1^\infty \frac{1}{\xi^*-\lambda}e^{-ik(\lambda+\lambda_1)}d\lambda\right\}d\xi^* \tag{42}$$

where

$$\Phi_\Gamma(k)=\frac{B_1(k,k_1)+B_2(k,k_1)}{1+k^2\left\{-\frac{\pi}{2}\left[H_1^{(2)}(k)+iH_0^{(2)}(k)\right]-e^{ik}/(ik)^2\right\}^2} \tag{43}$$

$$B_1(k,k_1)=4\pi^2[I_0^2(k_1)-I_1^2(k_1)]\Phi_G(k),\quad B_2(k,k_1)=-4\pi^2 I_0(k_1)I_1(k_1)\Phi_F(k)$$

In the same way, the auto-correlation functions of pressure distribution, $R_{\Delta p_a}(x^*, x_1^*, U\tau)$, and lift, $R_L(U\tau)$, can also be obtained from $R_{\gamma_a}(x^*, x_1^*, U\tau)$ as follows:

$$R_{\Delta p_a}(x^*, x_1^*, U\tau)=(\rho U)^2\left[R_{\gamma a}(x^*, x_1, U\tau)-\frac{\partial^2}{\partial(U\tau)^2}\int_{-1}^{x_1^*}d\xi_1^*\int_{-1}^{x^*}R_{\gamma a}(\xi^*, \xi_1^*, U\tau)\,d\xi^*\right] \tag{44}$$

$$R_L(U\tau)=b^2\int_{-1}^{1}dx_1^*\int_{-1}^{1}R_{\Delta p_a}(x^*, x_1^*, U\tau)\,dx^* \tag{45}$$

The Fourier transformations of equations (44) and (45) reduce the power spectral functions, which are

$$\Phi_{\Delta p_a}(x^*, x_1^*, k)=\int_0^\infty R_{\Delta p_a}(x^*, x_1^*, U\tau)\,e^{-ik(U\tau)}\,d(U\tau) \tag{46}$$

$$\begin{aligned}\Phi_L(k)&=\int_0^\infty R_L(U\tau)\,e^{-ik(U\tau)}d(U\tau)\\&=(\rho bU)^2\left[1-\left(\frac{3}{2}k^2\right)^2\right]\left[B_2(k,k_1)+B_2(k,k_1)\right]\\&-\frac{12(\pi k)^2}{k_1}\left[(I_0-I_1)I_1\Phi_G(k)-\frac{k_1}{2}\left\{\frac{I_0I_1}{k_1}\ (I_0-I_1)^2\right\}\Phi_F(k)\right]\\&-\left(\frac{2\pi k}{k_1}\right)^2\left[I_1^2\Phi_G(k)-I_1(2I_1-k_1I_0)\,\Phi_F(k)\right.\\&-k^2\left[\frac{\pi}{2}\{H_1^{(2)}(k)+iH_0^{(2)}(k)\}+\frac{e^{-ik}}{ik}\right]^2\Phi_\Gamma(k,k_1)\\&+\left(\frac{3k^2}{2}\right)^2\left[H_1^{(2)}(k)+iH_0^{(2)}(k)\right]^2\Phi_\Gamma(k,k_1)\\&-i\cdot3k^3\left[H_1^{(2)}+iH_0^{(2)}(k)\right]\left[\frac{\pi}{2}2H_1^{(2)}(k)-\frac{i}{k}e^{-ik}\right]\Phi_\Gamma(k,k_1)\\&-k^2\left[\frac{\pi}{2}\,2H_1^{(2)}(k)-\frac{i}{k}e^{-ik}\right]^2\Phi_\Gamma(k,k_2)\end{aligned} \tag{47}$$

where $I_0=I_0(k_1)$, $I_1=I_1(k_1)$

Since the frequency transfer function of the lift are defined as $\Phi_L(k)/[(2\pi\rho bU)^2\,\Phi_{wG}(k)]$, it can be obtained from equation (47) and the power spectral function of gust w_G. Figure 14 shows the frequecny transfer functions of the lift, in which k_1 is a parameter.

3.2. Experiemnts

The experiments for determining the response of a wing to random gusts is performed by means of the same apparatus as the sinusoidal gusts. The different

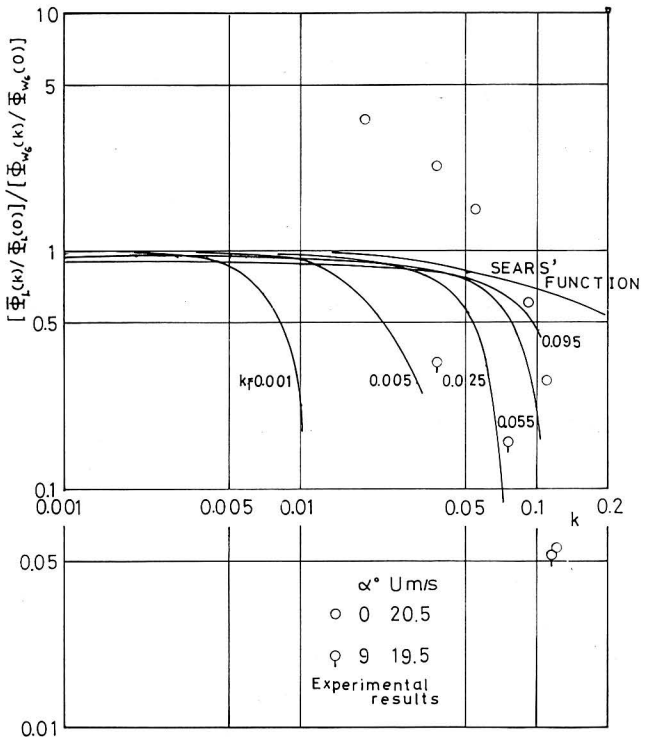

Fig. 14. Frequency transfer function

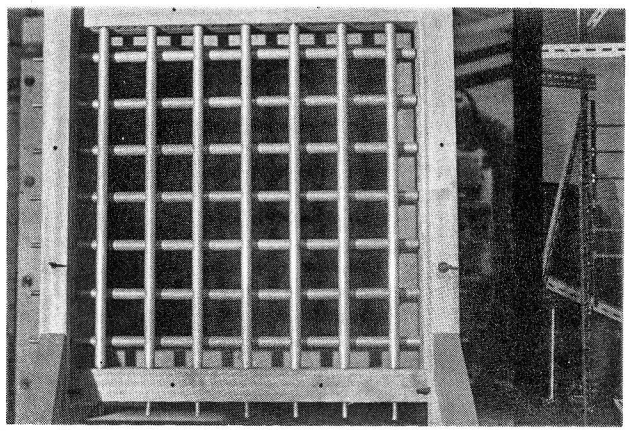

Fig. 15. Coarse grid

apparatus in this case was a coarse grid which generates the random gust in place of the sinusoidal gust (see figure 15).

3.2.1. Experimental Apparatus

The grid which was used for generating the random gust was constructed by

a number of circular cross-sectional bars which were framed with equal distances and were arranged to be normal to each other (see figure 15). The diameter of a bar is 20 mm and the distance between neighboring bars is 90 mm (mesh is 4.5). The airflow passing through the grid is the gusty wind and the input to a model wing. The position of a model wing is chosen at 600 mm downstream of the gird, where the characteristics of the flow became homogeneous and isotropic in our experiments.

The other experimental apparatus used is almost the same as that of the sinusoidal gust case. The recorder, however, in this case was a magnetic tape recorder with 4-channels.

3.2.2. Experimental Results

In this case, parameters of experiments are the velocity of uniform flow, U, and the angle of attack of the airfoil, α. The variations of the parameters in our experiments are as follows:

U: 10 and 20 m/s

α : 0, 3, 6, 9°

Since the data which were recorded by the magnetic tape are random, it is necessary to treat them by statistical methods. For this purpose the digital computer was utilized after converting the analog data into digital ones by A-D converter. The block diagram of these systems is shown in figure 16.

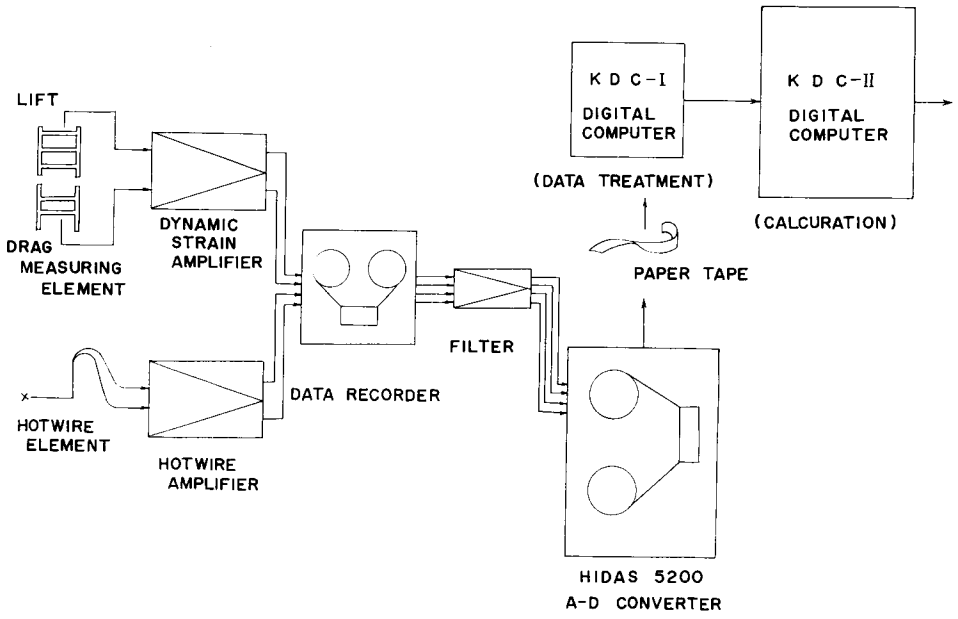

Fig. 16. Block diagram

The recording speed of the tape recorder was 30 inch/sec, and the reproducing speed was 3 inch/sec. The number of sampling points was 1500 and the speed was 1500 points per second. Therefore, the time interval between a datum and its neighbor was 0.0003 second.

The following equations are used to obtain the response of a wing, i.e.

(a) Correlation function $R(\tau)$

$$R(\tau)=\lim_{T\to\infty}\int_0^T y(t)\,y(t+\tau)\,dt \tag{48}$$

(b) Power spectral density function $\Phi(k)$

$$\Phi(k)=\frac{1}{R(0)}\left[\frac{2}{\pi}\int_0^\infty R(\tau)\ \cos\ (k\tau)\,d\tau\right] \tag{49}$$

(c) Frequency transfer function $T(k)$

$$T(k)=\Phi_L(k)/\Phi_{wg}(k) \tag{50}$$

where, $\Phi_L(k)$ indicates the power spectral function of lift.

Since the numbers of digitalized data were about 1500, the correlation functions were calculated by

$$R(\tau)=\sum_{i=1}^{n} y_i\cdot y_{i+\tau}\cdot\Delta t,\quad R(0)=\sum_{i=1}^{n} y_i{}^2\Delta t \tag{51}$$

$$\Delta t=0.0003\ \text{sec}$$

for the lift and the drag, and

$$R(\tau)=\sum_{i=1}^{n/2}\ (y_i-y_{i+1})\ \ (y_{i+\tau}-y_{i+\tau+1})\,\Delta t \tag{52}$$

for the gust, where n is the number of data, and τ is the correlation interval, which

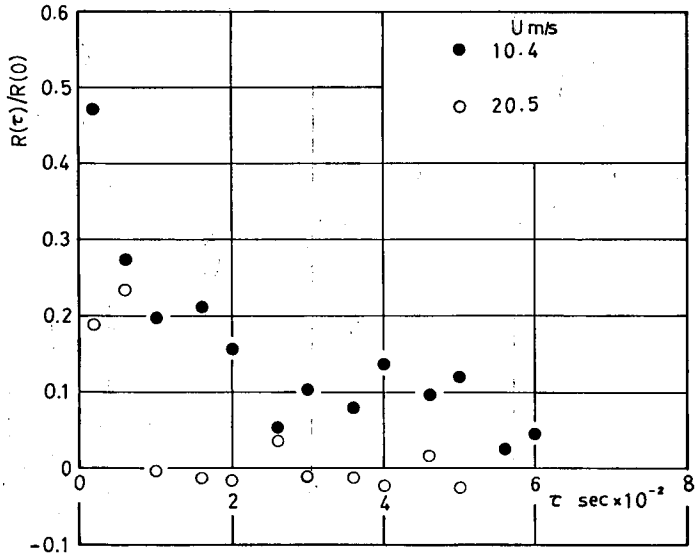

Fig. 17. Correlation of gust

is equal to Δt as the minimum value and 200 Δt as the maximum value. The power spectral functions were obtained by integration of $R(\tau)$ by numerical method.

(1) Gust

The auto-correlation functions and the power spectral functions of the gusts

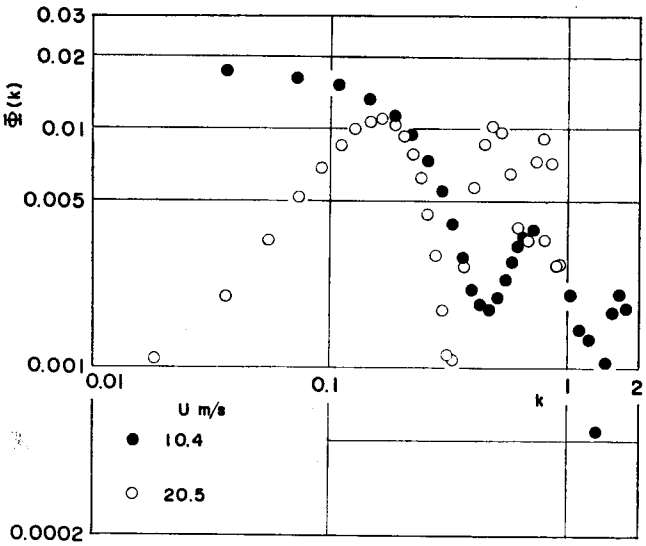

Fig. 18. Power spectrum of gust

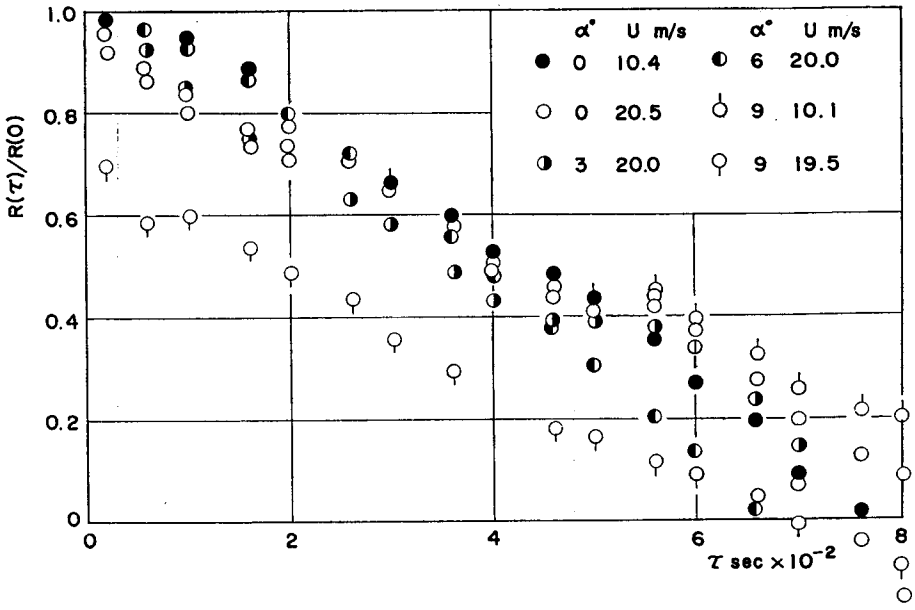

Fig. 19. Correlation of lift

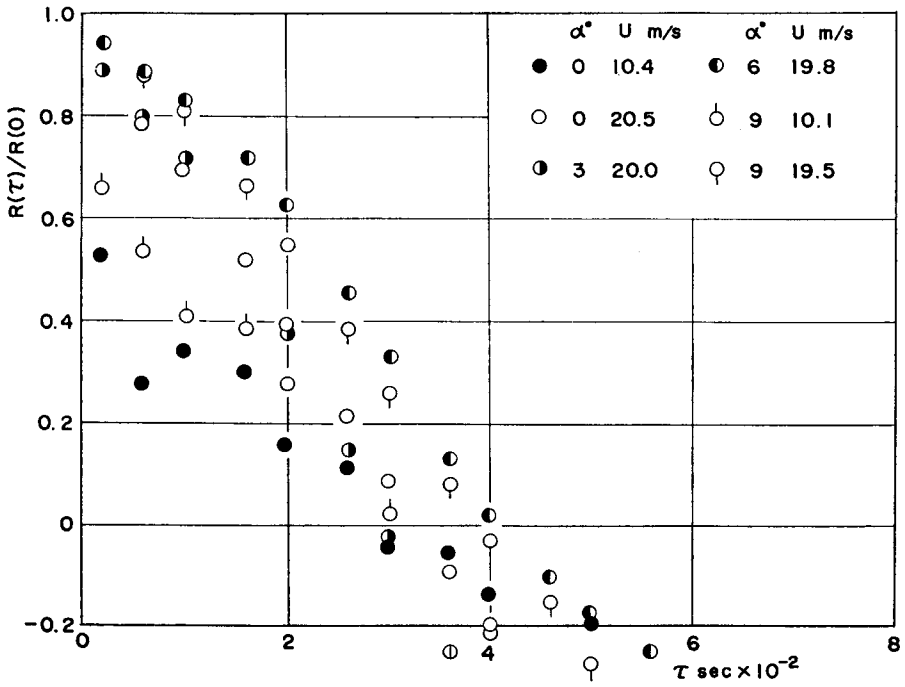

Fig. 20. Correlation of drag

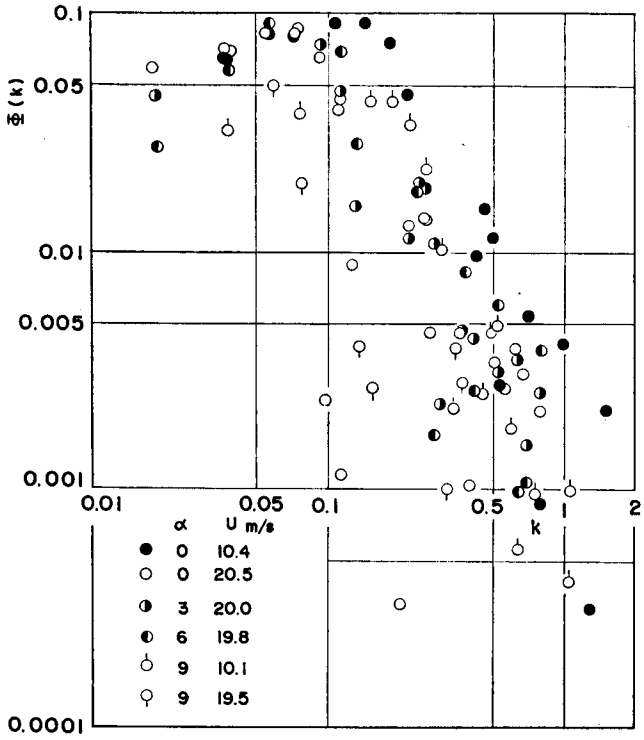

Fig. 21. Power spectrum of lift

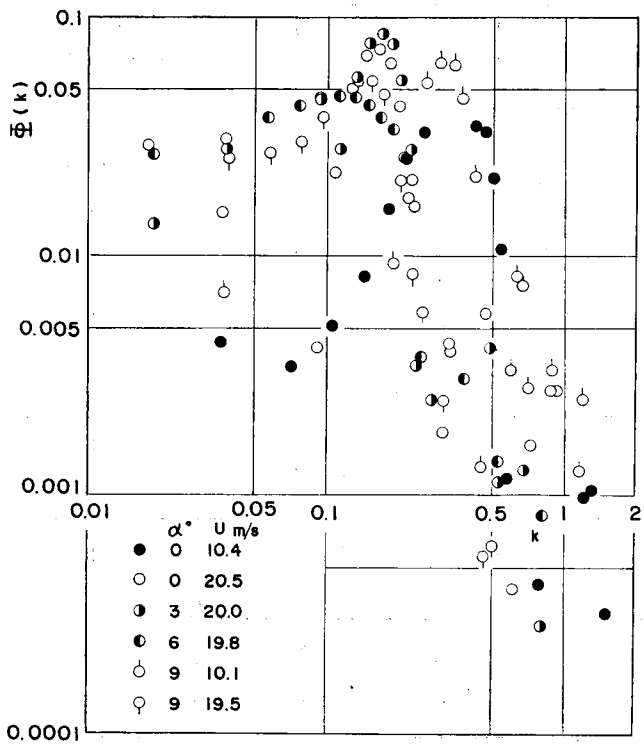

Fig. 22. Power spectrum of drag

are shown in figure 17 and 18 respectively. The gusts are supposed to be correlated only slightly, but the power spectral function of the case of U=10 m/s agree well with the theoretical value of homegeneous and isotropic turbulence, where $b/L \simeq 0.7$. However the case of U=20 m/s does not agree with the theoretical value at the small value of k.

(2) Lift and drag

Figure 19, and 20 show the auto-correlation function of lift and drag respectively. The correlation of lift seems to be larger than that of the gust. The power spectral functions of lift and drag are shown in figure 21 and 22. Though the points are scattered considerably, the changes due to α are also considered to be small.

(3) Frequency transfer function

For convenience, the values of correlation functions and power spectral functions were shown by the calculated values using the digitalized data. However, the frequency transfer functions can be obtained by the power spectral density functions, and it is given by

$$T(k) = \frac{\Phi_L(k)/\Phi_L(0)}{(2\pi\rho bU)^2 \Phi_{wa}(k)/\Phi_{wa}(0)} \tag{53}$$

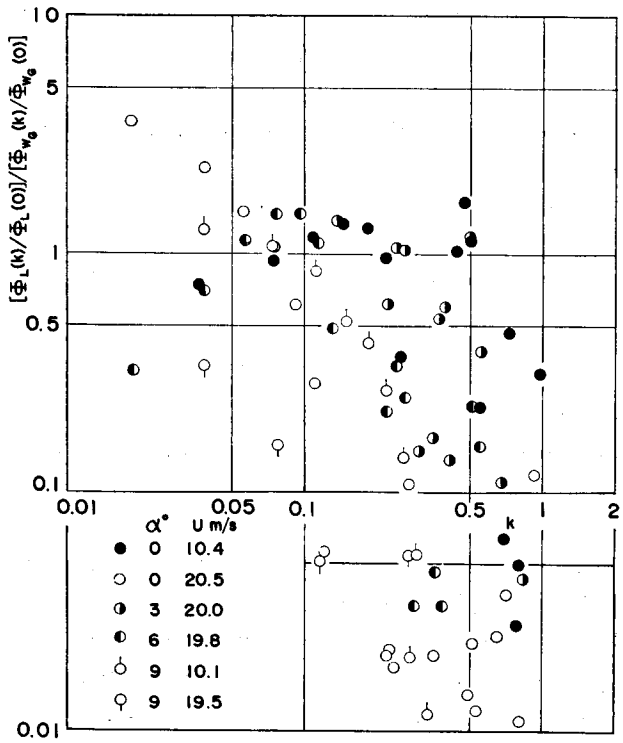

Fig. 23. Frequency transfer function

As shown in figure 23 the frequency transfer functions are also scattered considerably, but the tendency to k is considered to have a steeper slope than that of Sears' function.

3.3. Considerations

When the response to random gusts is discussed, Sears' gust function cannot be used as the frequency transfer function. In this report we have obtained the transfer function based on the assumptions that the integral equation for circulation distribution can be solved by Söhngen's formula in the random case too. The result seems to agree with experimental values pretty well. As shown in figure 14, it is found that the inclination of curves tends to that of Sears' function, when the parameter k_1 $(=b/L)$ becomes large.

In this diagram, it seems that the experimental results and the theoretical curves agree well at $k_1=0.01\sim0.05$, but it is not so clear because the scale of turbulence L for the coarse grid was undetermined. L is supposed to be rather small by the measurements of gust.

When k becomes large, the theoretical values increase abruptly. This is because the assumption of the relation between circulations and wake vortices

was the same as sinusoidal case. Further, it is considered in this report that the random gust is two-dimensional, but the phase differences along the span should be included.

The additional reasons why the experimental values scatter considerably are considered to be as follows:

(a) Dismatching of impedance between strain gage amplifier and tape recorder may make S/N ratio to be worse.

(b) Sampling points were too few for the larger value of k.

4. Conclusion

In this report the reasponse chracteristics of a two-dimensional, rigid wing to the gusts are investigated experimentally. The gusts treated here are the normal gusts which vary normally to the main flow sinusoidally and randomly.

The model wing used in the experiments has NACA-0012 airfoil section. In the case of the sinusoidal gust, the experimental results agree pretty well with the case of oscillating wings, but it is found that the absolute value of lift variations are less than those of Sears' function and phase differences are large. In the case of random gust, it is found that the inclination of the frequency transfer functions of the lift are different from those of Sears' function.

Analyses have been made for both the sinusoidal case and the random case. In the former case thickness effects are particularly investigated and for the latter case the frequency transfer function is obtained from the power spectral functions of circulations. The difference between the experimental results and the calculated ones are also discussed.

5. Notations

a_j	coefficient of mean camber line
A_{ij}	coefficient of simultaneous equation for circulation
b	half length of chord
d	diameter of coarse grid
G_r	coefficient of circulation distribution
h	strength of source
I_0, I_1	modified Bessel functions of first kind
J_0, J_1	Bessel functions of first kind
k	reduced frequency $(=b\omega/U)$
k'	reduced frequency of turbulence $(=L\omega/U)$
k_1	parameter of random gust response $(=b/L)$
K_0, K_1	modified Bessel functions of second kind

l interval length of coarse grid
L lift or scale of turbulence
Δ_{p_a} pressure distribution of airfoil
$R(\tau)$ correlation function
$S(k)$ Sears' function
t time
u, w velocity components
U main flow velocity
w_G gust velocity (normal)
x, z reference axes along U and normal to U
α angle of attack
γ_a circulation distribution on airfoil
γ_w circulation distribution of wake
Γ over-all circulation of airfoil
ξ, ζ distances of circulation and source distribution
ω natural frequency
Ω $=\Gamma'/b$
$\Phi(k)$ power spectral function
ϕ, θ converted variables from x and ξ
ρ density of air
τ half thickness of airfoil or correlation interval

$$\Phi_F(k') = \frac{2L}{\pi} \frac{1}{1+k'^2}$$

$$\Phi_G(k') = \frac{L}{\pi} \frac{1+3k'^2}{(1+k'^2)^2}$$

6. Refferences

1) R.L. Bisplinghoff, H. Ashley and R.L. Halfman ; Aeroelasticity, 1957, Addison-Wesley Pub. Co.
2) B. Etkin ; Dynamics of Flight, 1959, John Wiley & Sons Inc.
3) J.O. Hinze ; Turbulence, 1959, McGraw-hill Inc.
4) I.A. Abbot and A.E. von Doenhoff ; Theory of Wing Sections, 1959, Dover Pub. Inc.
5) W.R. Sears ; Some Aspects of Non-stationary Airfoil Theory and Its Practical Application, Jour. Aeronaut. Sci., vol. 8, 1941
6) Y.L. Luke and M.A. Dengler ; Tables of the Theodorsen Circulation Function for Generalized Motion, Jour. Aeronaut. Sci. July, 1951'
7) R.L. Halfman ; Experimental Aerodynamic Derivatives of a Sinusoidally Oscillating Airfoil in Two-Dimensional Flow, NACA Rep. 1108, 1949
8) R.J. Hakkinen and A.S. Richardson ; Theoretical and Experimental Investigation of Random Gust Loads, Part I, NACA TN 3878, 1957
9) H. Press and J.C. Houbolt ; Some Applications of Generalized Harmonic Analysis to Gust Loads on Airplanes, Jour. Aeronaut. Sci. 1955

10) J.M. Eggleston and F.W. Diederich ; Theoretical Calculation of the Power Spectra of the Rolling and Yawing Moments on a Wing in Random Turbulence, NACA TN 3864, 1956
11) L.T. Filotas ; Theory of Airfoil Response in a Gusty Atmosphere, Part I, UTIAS Rep. No. 139, 1969
12) L.T. Filotas ; Theory of Airfoil Response in a Gusty Atmosphere, Part II, UTIAS Rep. No. 141, 1969
13) H. Press, M.T. Meadows and I. Hadlock ; A Reevaluation of Data on Atmospheric Turbulence and Airplane Gust Loads for Application in Spectral Calculation, Rep. NACA 1272, 1957
14) D.S. Whitehead ; Force and Moment Coefficients for Vibrating Aerofoils in Cascade, R&M No. 3254, 1962